

Identification of wave drift force QTFs for the INO WINDMOOR floating wind turbine based on model test data and comparison with potential flow predictions

Nuno Fonseca, Maxime Thys, Petter Andreas Berthelsen
SINTEF Ocean

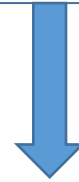
EERA DeepWind'2021
13 – 15 January 2021

WINDMOOR



Objectives

- Identify QTFs of wave drift loads from model test data
- Assess the influence of seastate severity and wave-current effects on the QTFs
- Assess quality of numerical predictions by full 2nd order potential flow calculations



Establish a basis for assessing improved
force models to predict wave drift loads

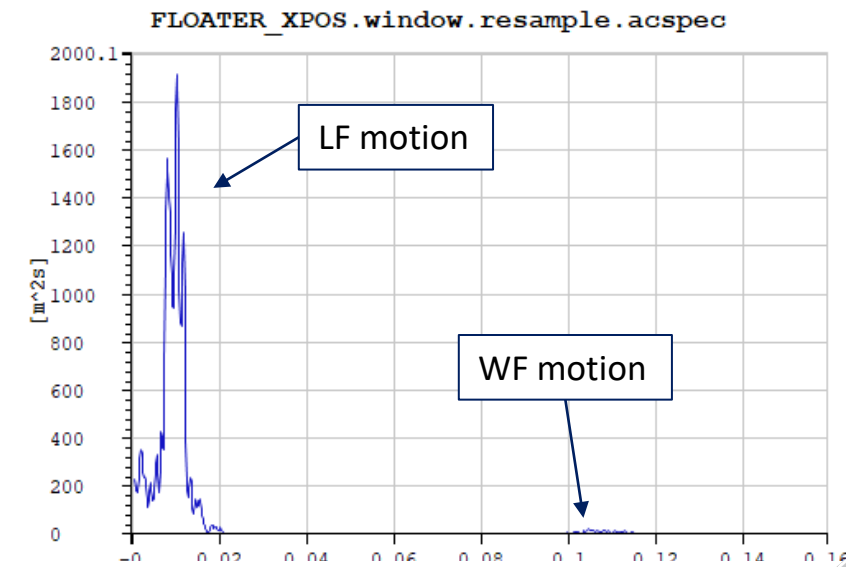
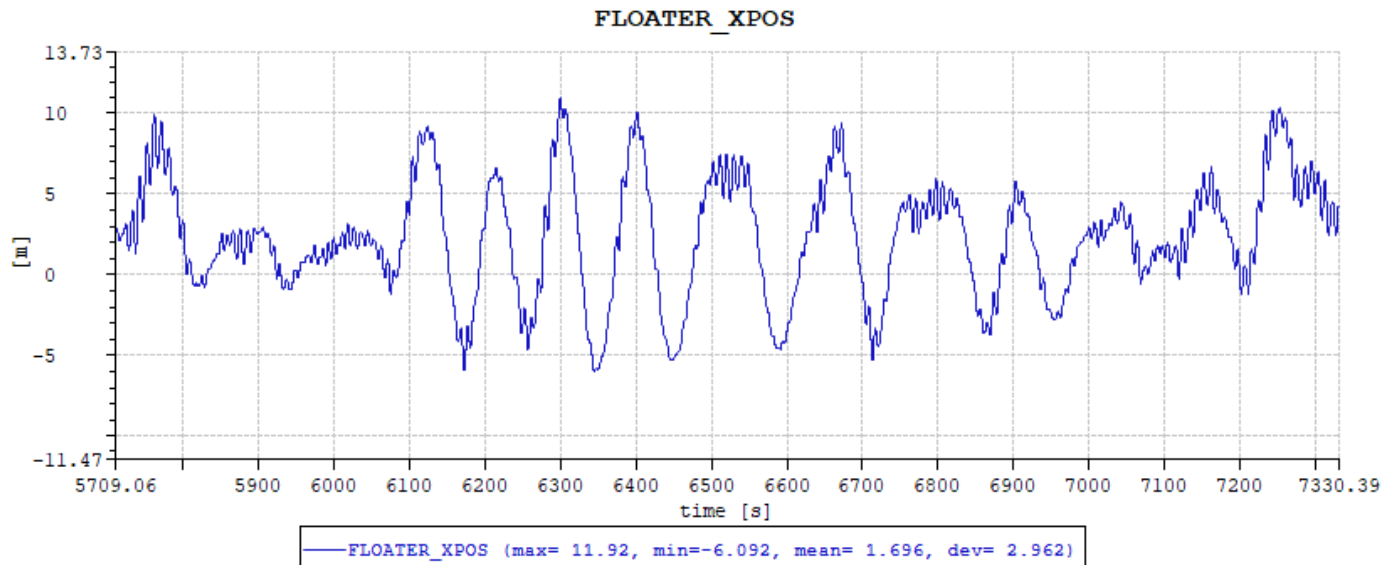
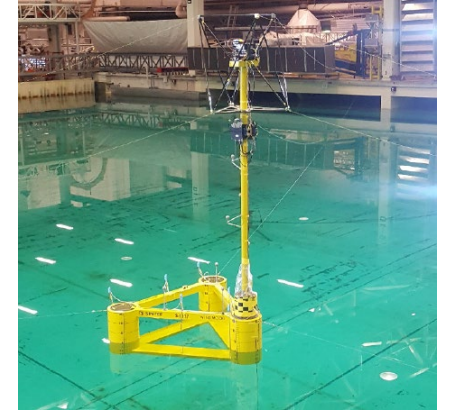


Why

LF motions:

- Large contribution to mooring line loads.
- Large uncertainty in numerical predictions.

INO WindMoore test 4230: $H_s = 6.2$ m, $T_p = 9.0$ s, $U_c = 0$, heading = 0



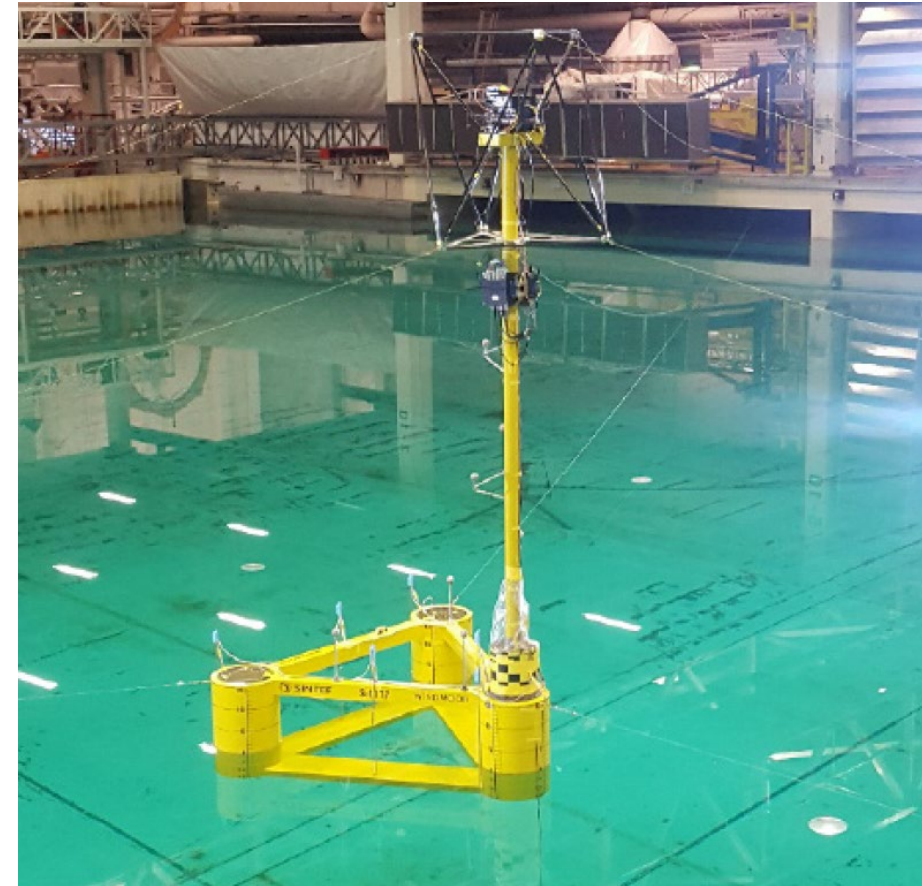
1. Case study

INO WINDMOOR semisubmersible is jointly designed by Inocean and Equinor.

Parameter	Unit	Value
Column diameter	[m]	15.0
Column height	[m]	31.0
Pontoon width	[m]	10.0
Pontoon height	[m]	4.0
Centre-centre distance	[m]	61.0
Draft	[m]	15.5
Displacement	[t]	14124
Long. centre of gravity (LCG)*	[m]	0.0
Trans. centre of gravity (TCG)*	[m]	0.0
Vert. centre of gravity (VCG)**	[m]	19.4
Long. metacentric height (pitch)	[m]	9.52
Transv. metacentric height (roll)	[m]	9.53
Roll radius of gyr. (Rxx)	[m]	43.6
Pitch radius of gyr. (Ryy)	[m]	44.0
Yaw radius of gyr. (Rzz)	[m]	29.9

* wrt the floater geometric center

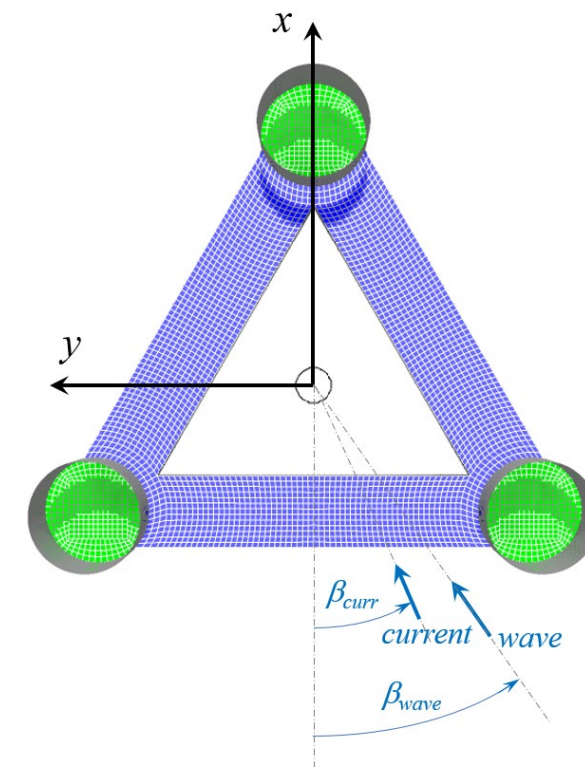
** wrt the baseline



2. Model tests

- Model tests in the Ocean Basin of SINTEF (February 2020)
- Model scale of 1:40
- Water depth of 150 m
- Horizontal mooring system
- Waves and current only
- JONSWAP seastates (long crested)
- 3 hours effective duration of the tests

Test no.	Heading (deg.)	Uc (m/s)	Hs (m)	Tp (s)	Gamma
4010	0	0	4.0	4.5-20	-
4210, 4222, 4223, 4224, 4225	0	0	3.7	7.0	4.90
4230, 4240, 4241, 4242, 4243, 4244	0	0	6.2	9.0	4.90
4270	0	0	3.7	12.0	1.00
4290, 4292	0	0	6.2	12.0	1.23
4662, 4670, 4673, 4674, 4675, 4676, 4677	0	0	11.0	12.0	4.90
4480	90	0	6.2	9.0	4.90
4490	90	0	6.2	12.0	1.20
4510, 4520, 4521, 4523, 4524, 4525	0	0	2.0	7.0	1.06
4560	0	0	15.0	14.0	4.90
4250, 4260, 4261, 4262, 4263	0	1.2	6.2	9.0	4.90
4340, 4350, 4351, 4352, 4353, 4354	0	1.2	11.0	12.0	4.90
4530	0	1.2	2.0	7.0	1.06



3. Method for identification of empirical QTFs

The floater motion may be represented by:

$$x(t) = x^{(0)} + x^{(1)}(t) + x^{(2)}(t) + E_x(t) \quad (1)$$

The slow drift oscillations which are assumed to be represented by a 1 DOF oscillator:

$$\ddot{x}^{(2)}(t) + 2\xi\omega_n\dot{x}^{(2)}(t) + \omega_n^2x^{(2)}(t) = \frac{1}{m}g^{(2)}(t) \quad (2)$$

The wave exciting forces are represented by an expansion similar to (1):

$$g(t) = g^{(0)} + g^{(1)}(t) + g^{(2)}(t) + E_g(t) \quad (3)$$

The quadratic component of the exciting force can be represented in terms of the Fourier transform of the wave elevation, $Z(f_n)$, and the complex wave force QTF, $H^{(2)}(f_m, f_n)$:

$$g^{(2)}(t) = \int_{-\infty}^{\infty} \int_{-\infty}^{\infty} [Z^*(f_m)Z(f_n)H^{(2)}(f_m, f_n)e^{i2\pi(f_m-f_n)t}]df_mdf_n \quad (4)$$

3. Method for identification of empirical QTFs

The Fourier transform of $g^{(2)}(t)$ gives:

$$G^{(2)}(f) = \int_{-\infty}^{\infty} [g^{(2)}(t) e^{-i2\pi f t}] dt, \quad f = (f_m - f_n) \quad (5)$$

The cross bi-spectrum of $g^{(2)}(t)$ with respect to $\zeta(t)$ is given by:

$$S_{\zeta\zeta g}(f_m, f_n) = \langle Z^*(f_m) Z(f_n) G^{(2)}(f_m - f_n) \rangle \quad (6)$$

Manipulation of equations (4), (5) and (6) leads to an expression for estimation of the QTF:

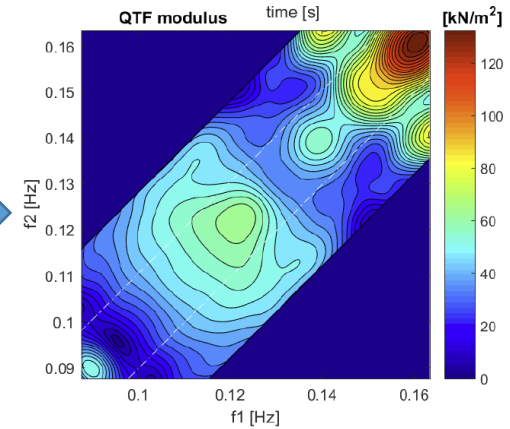
$$H^{(2)}(f_m, f_n) = S_{\zeta\zeta g}(f_m, f_n) / S_{\zeta\zeta}(f_m) S_{\zeta\zeta}(f_n) \quad (7)$$

where $S_{\zeta\zeta}(f)$ is the wave spectrum.

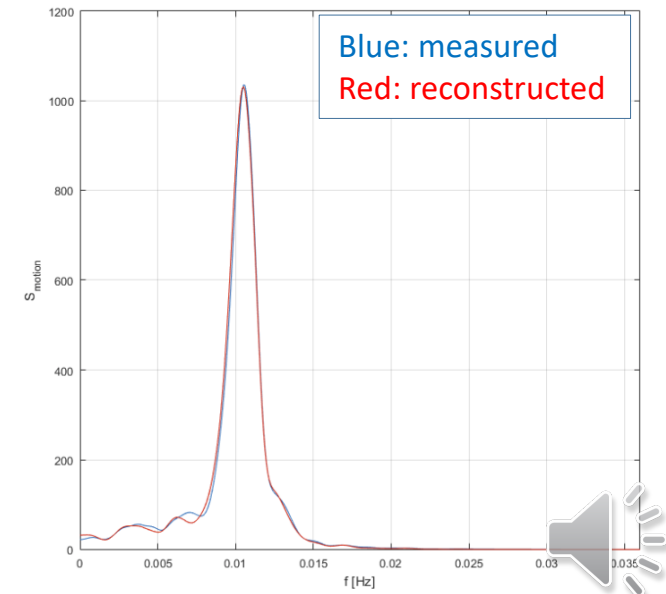
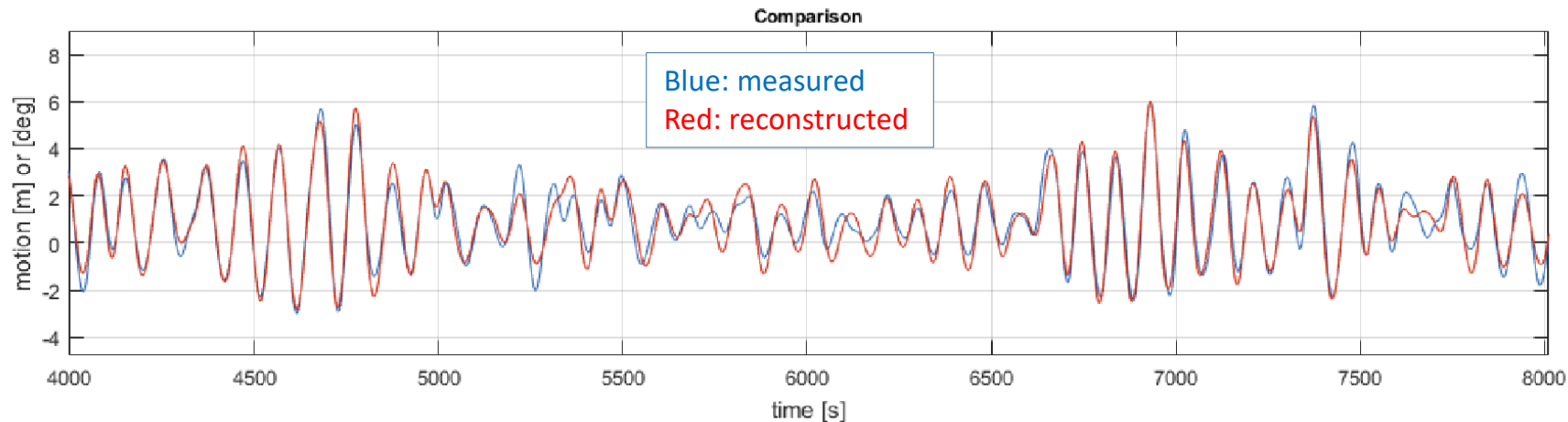
3. Method for identification of empirical QTFs

Two steps:

- (1) Identify 2nd order wave exciting force time history from measured LF motion signals;
- (2) Use the undisturbed incident wave elevation and the estimated 2nd order force, together with cross bi-spectral analysis, to identify the difference frequency wave exciting QTF matrix.



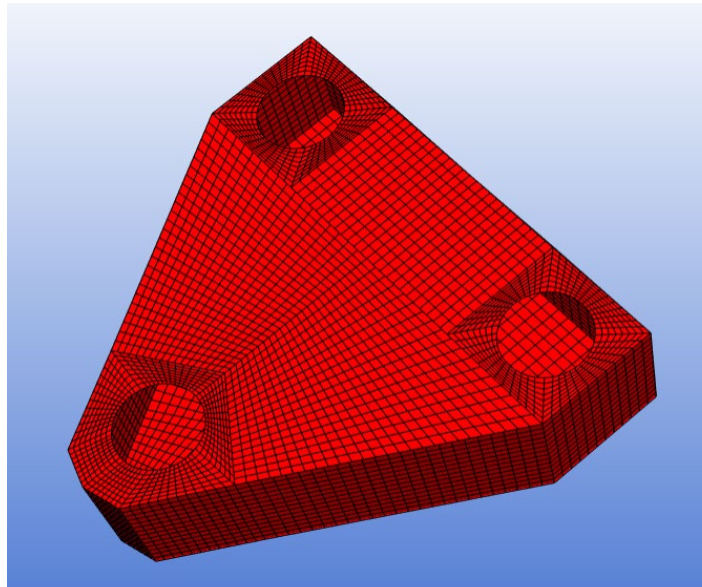
Case by case identification/validation: comparison between measured LF motions and reconstructed from the empirical QTF



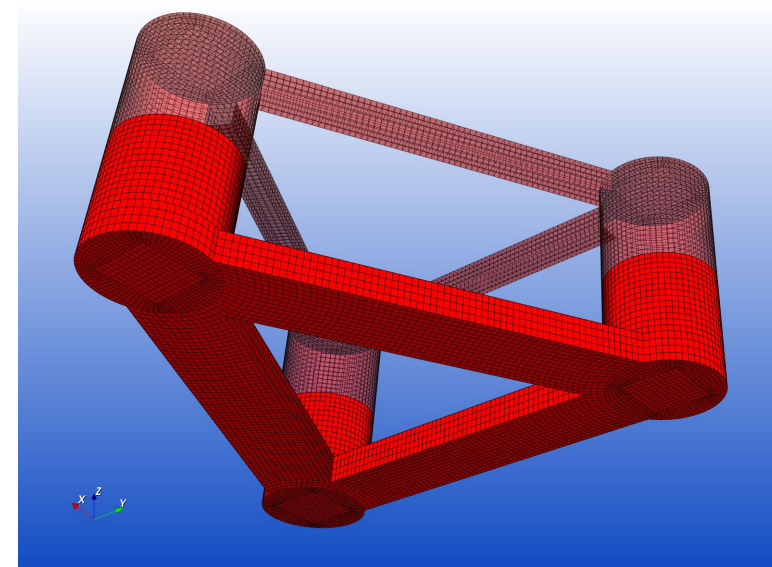
4. Numerical model

- Calculations performed with Hydrostar v8.1.
- Total of 17176 low order panels.
- Realistic additional damping coefficients used to calculate first order results.
- Wave drift load QTFs given by solution of the 2nd order boundary value problem (middle field method).

Control surface mesh (5964 panels)

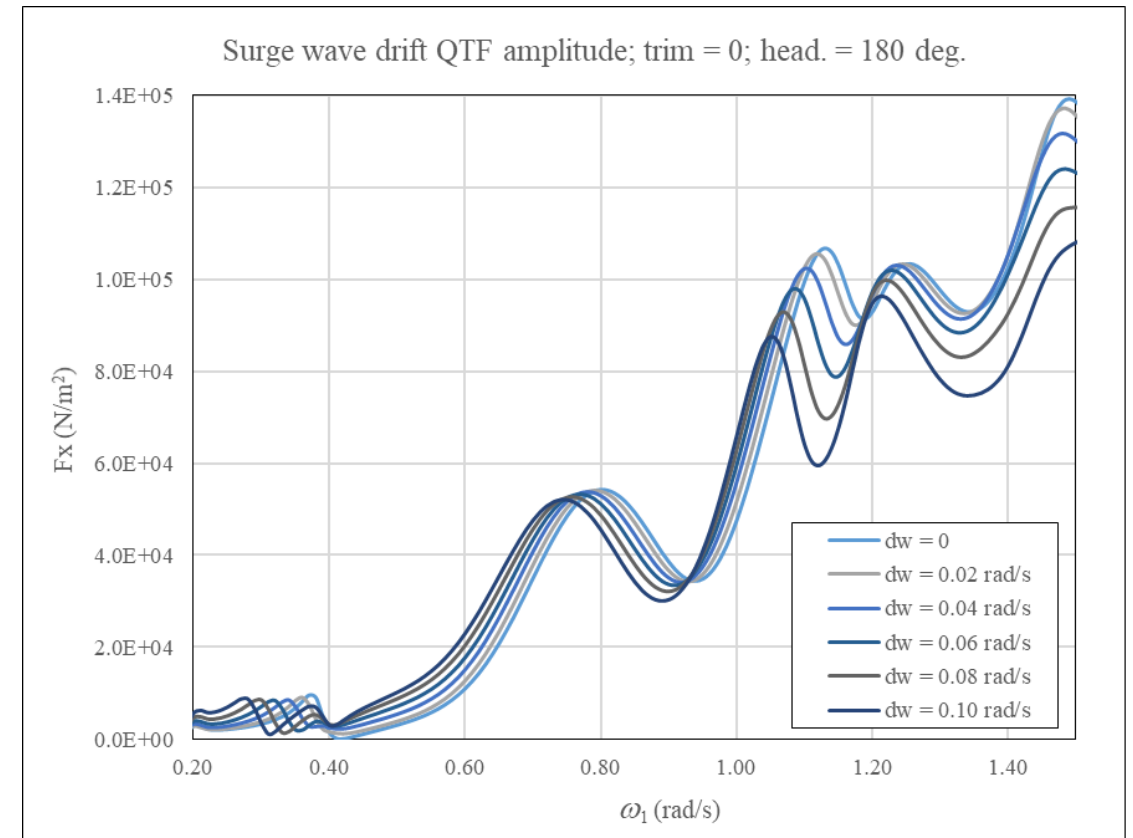
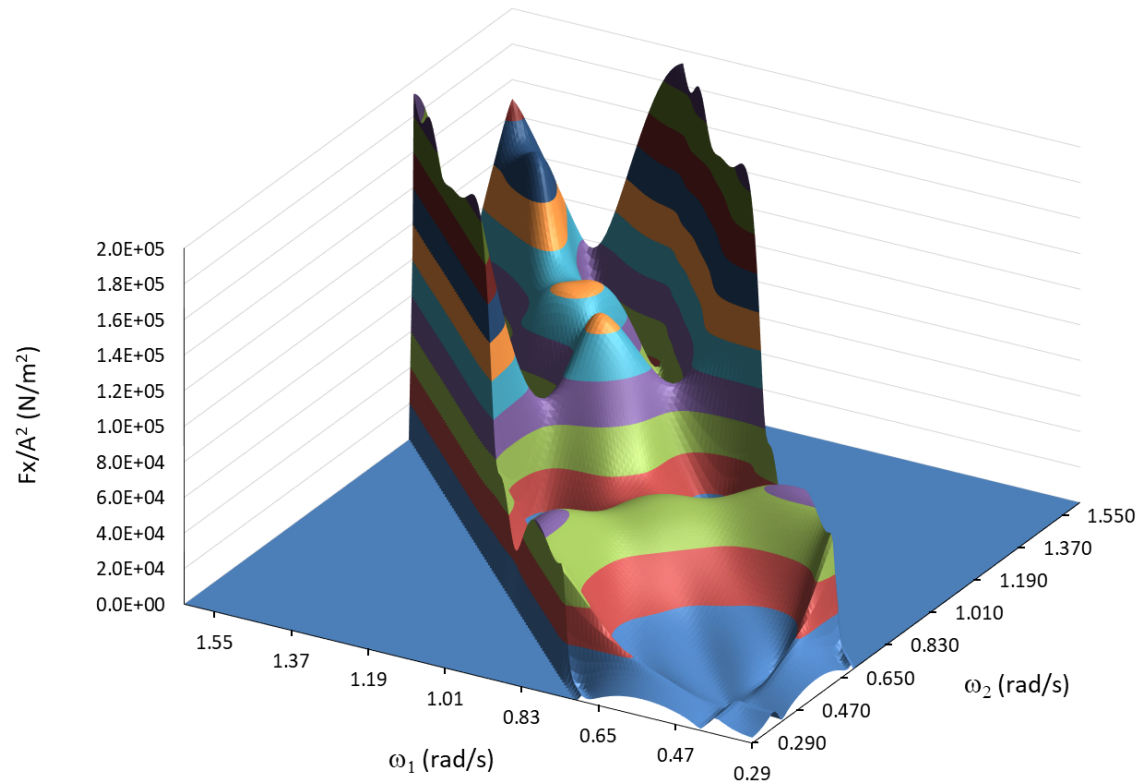


Hull mesh (11212 panels)



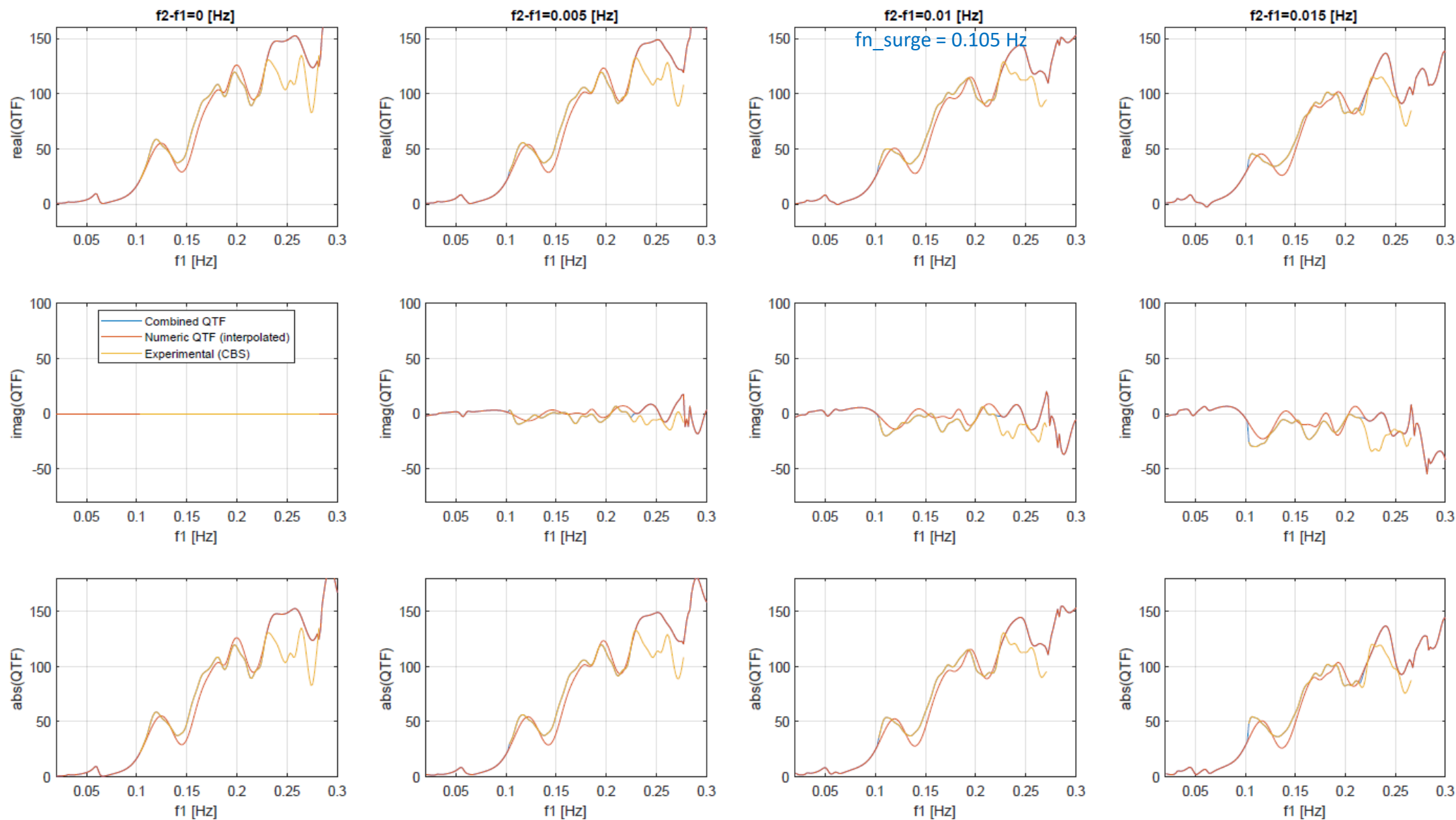
4. Numerical model

Surge LF wave load QTF amplitude, numerical



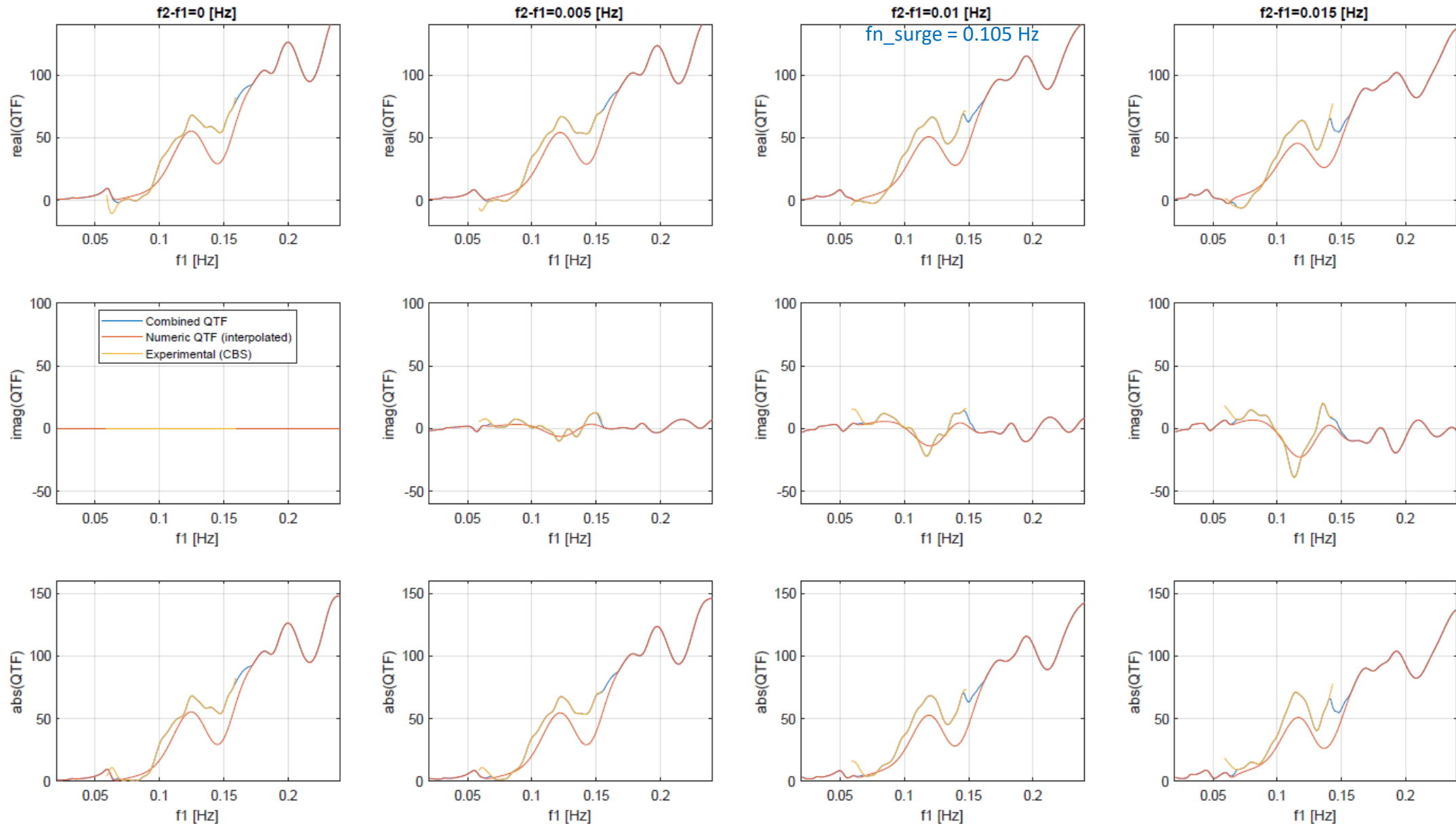
5. Results: surge QTF in small seastates ($H_s = 2.0$ m, $T_p = 7$ s, $U_c = 0$, Heading = 0 deg)

Force in X-dir, Direction = 0 deg., Test nr. = 4510 to 4525



5. Results: surge QTF in moderate/high small seastates ($H_s = 6.2$ m, $T_p = 12$ s, $U_c = 0$, Heading = 0 deg)

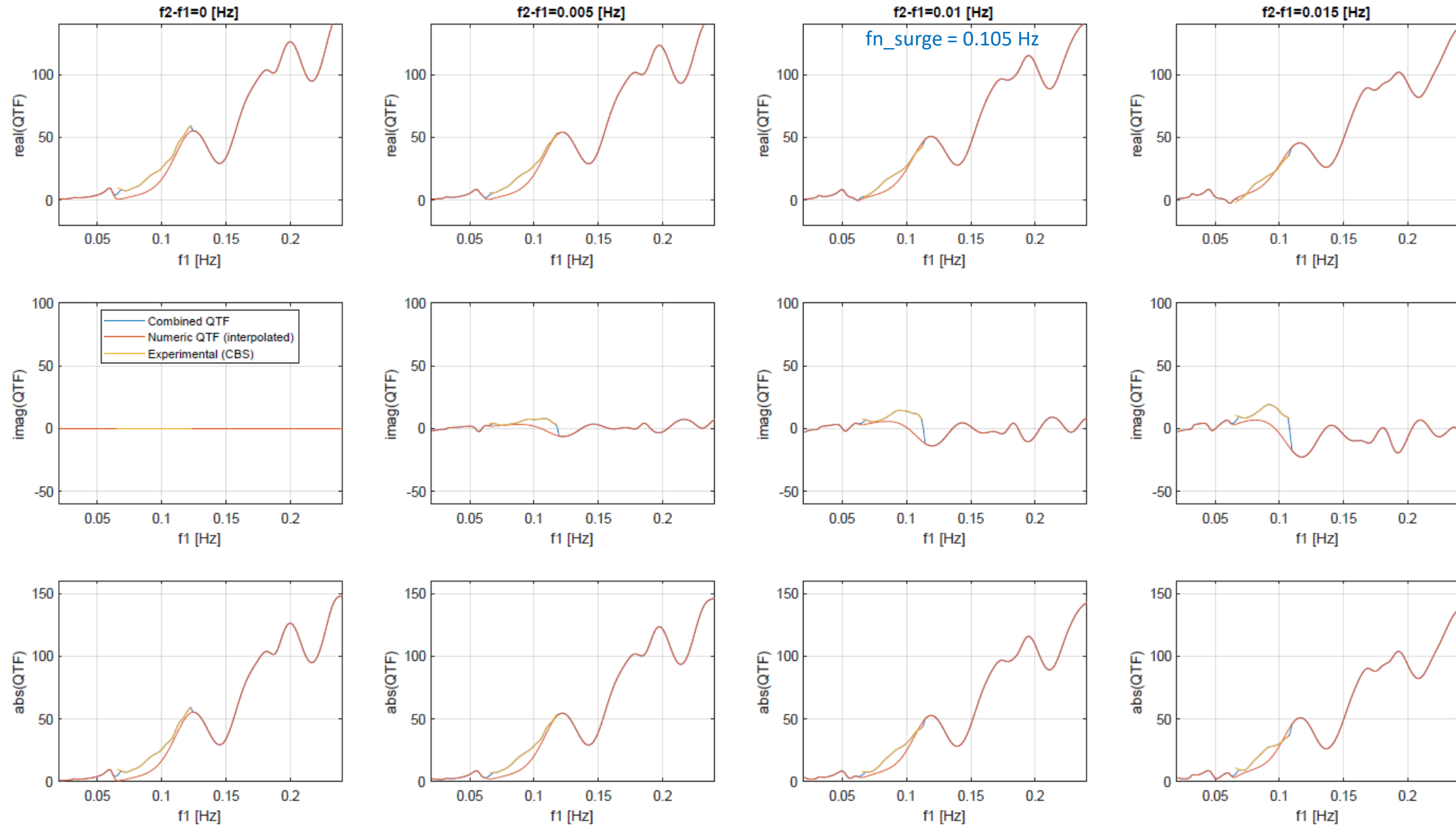
Force in X-dir, Direction = 0 deg., Test nr. = 4290 to 4292



5. Results: surge QTF in moderate/high small seastates ($H_s = 11.0$ m, $T_p = 12.0$ s, $U_c = 0$, Heading = 0 deg)

INDMOOR

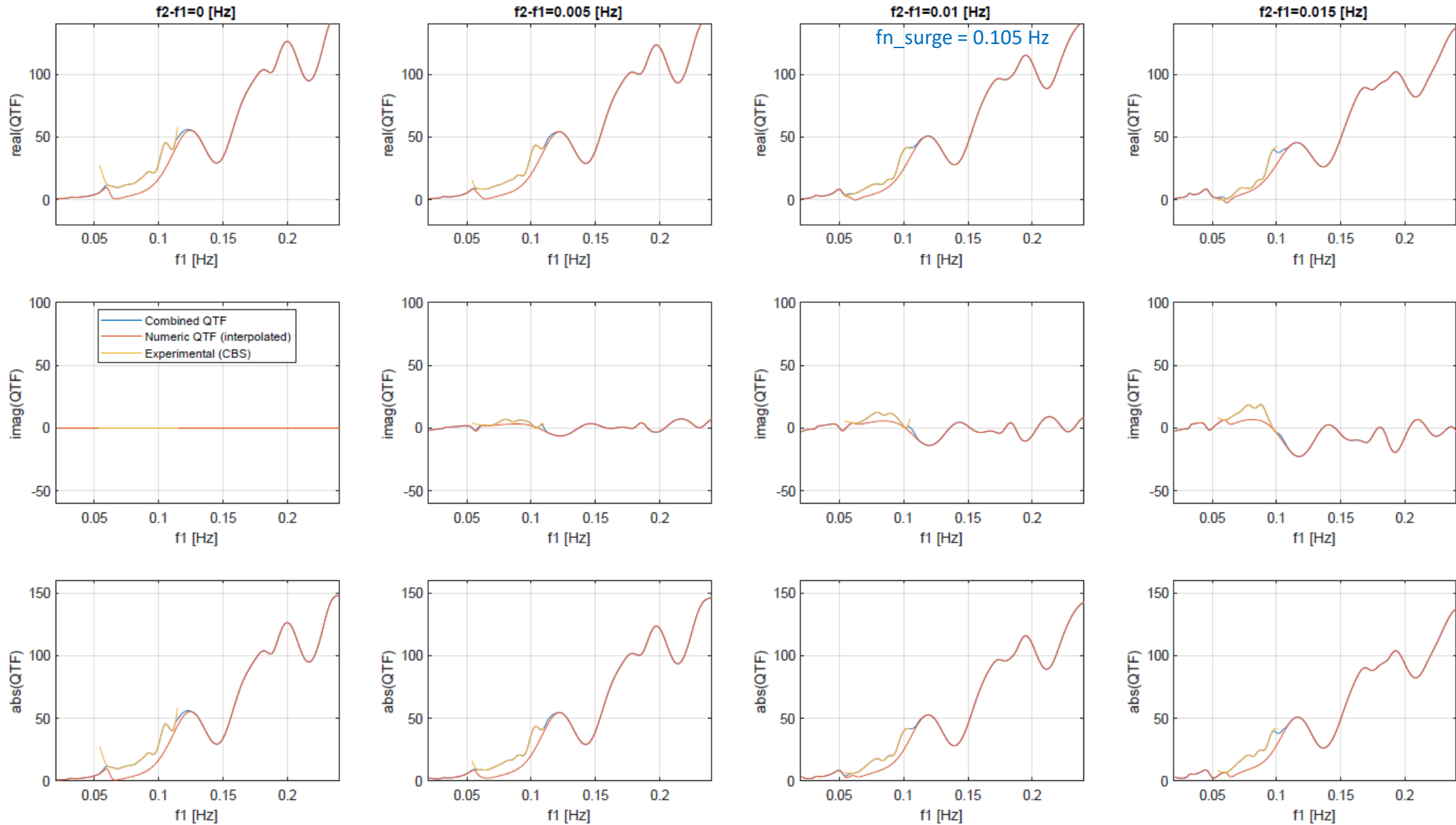
Force in X-dir, Direction = 0 deg., Test nr. = 4662 to 4677



5. Results: surge QTF in moderate/high small seastates ($H_s = 15.0$ m, $T_p = 14$ s, $U_c = 0$, Heading = 0 deg)

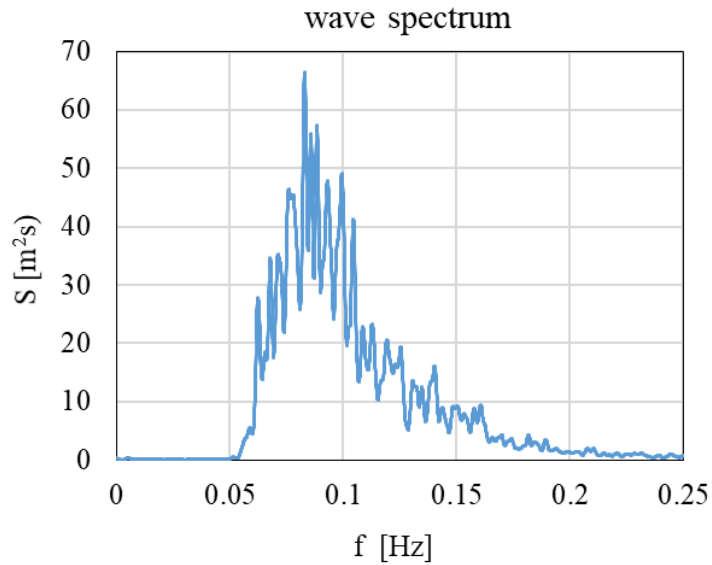
WINDMOOR

Force in X-dir, Direction = 0 deg., Test nr. = 4560

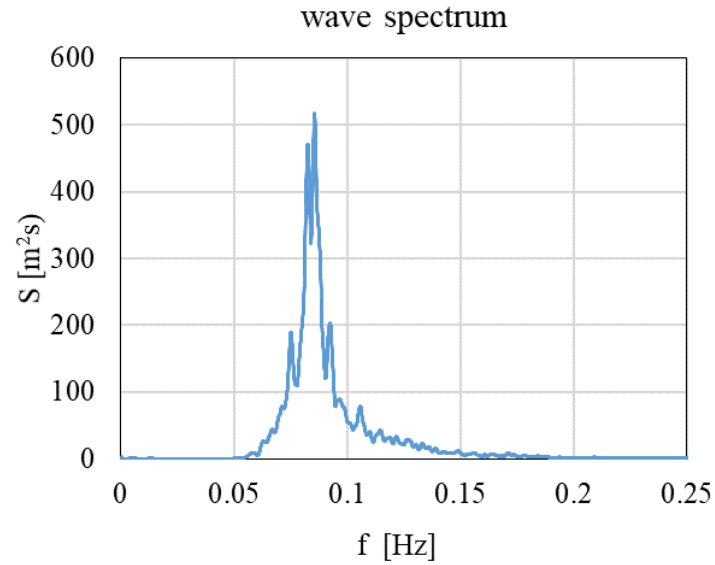


5. Results: surge QTF in moderate/high small seastates

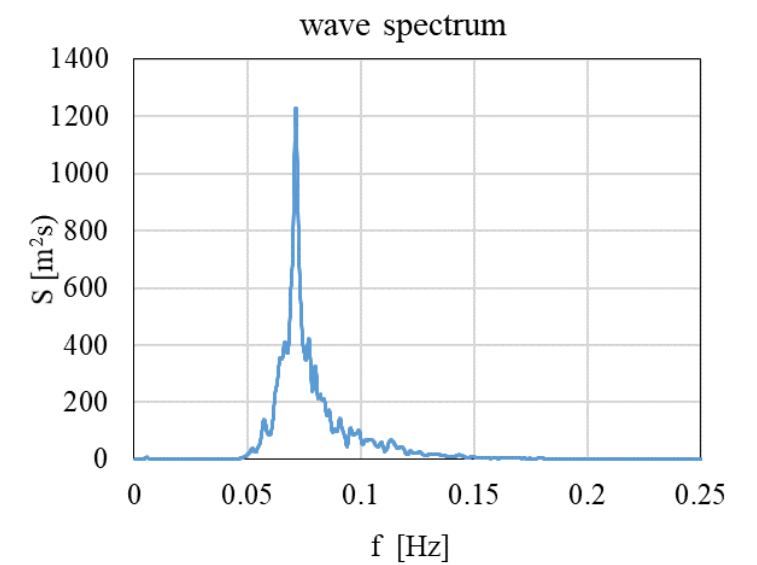
$H_s = 6.2$ m, $T_p = 12$ s, $\gamma = 1.23$



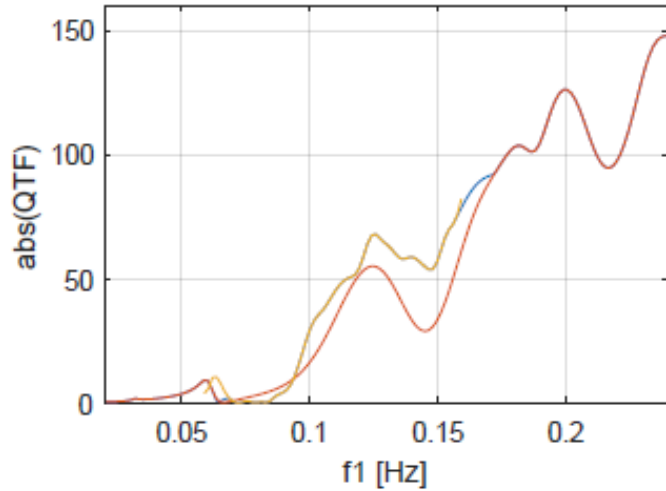
$H_s = 11$ m, $T_p = 12$ s, $\gamma = 4.9$



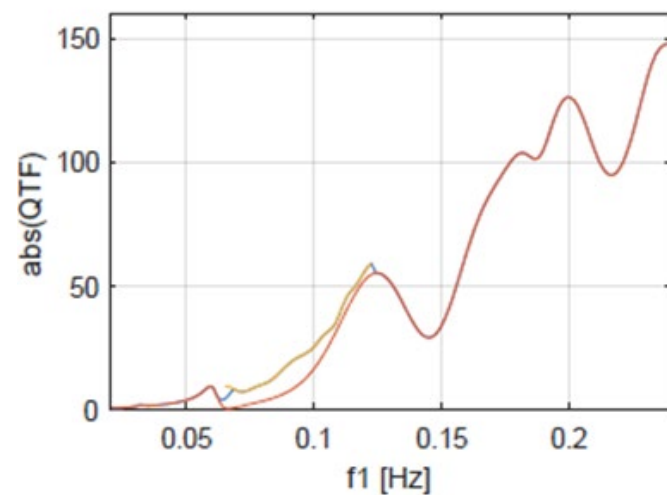
$H_s = 15$ m, $T_p = 14$ s, $\gamma = 4.9$



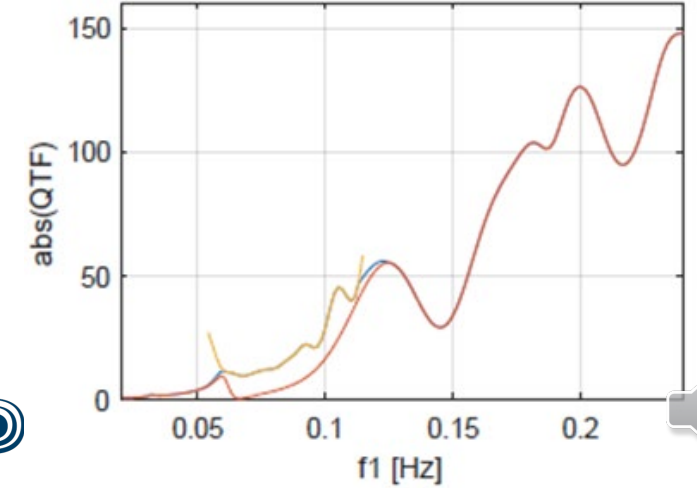
Surge QTF modulus, $df = 0$



Surge QTF modulus, $df = 0$



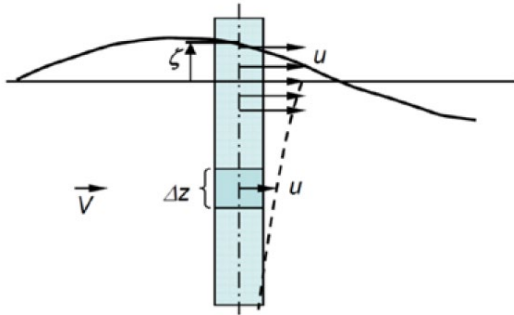
Surge QTF modulus, $df = 0$



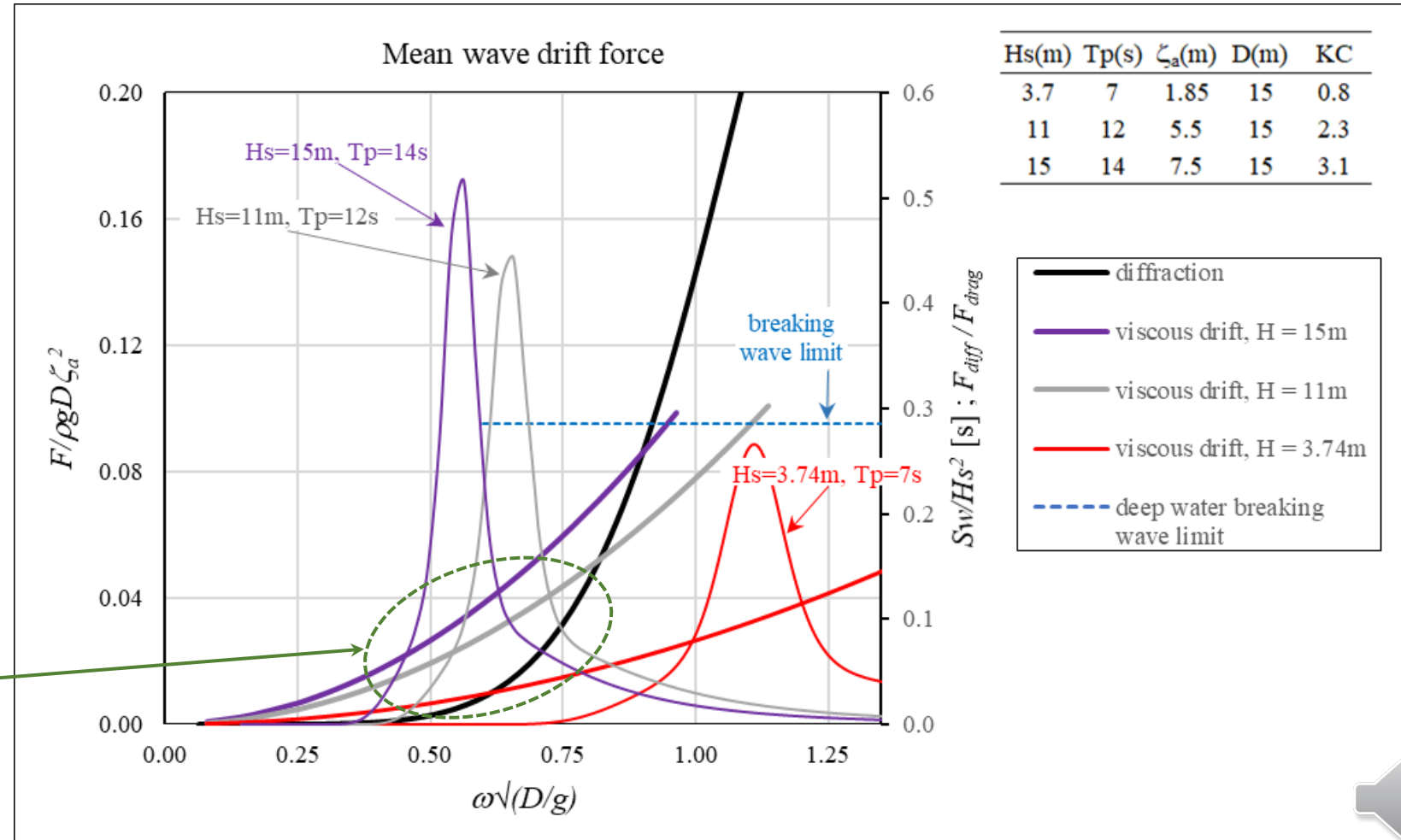
5. Results: discussion of empirical vs numerical QTFs

Mean drag force over one wave cycle
according to Morison's term with $C_d = 1.0$:

$$F_{drag} = (2/3\pi)\rho DC_D \zeta_a^3 \omega^2$$



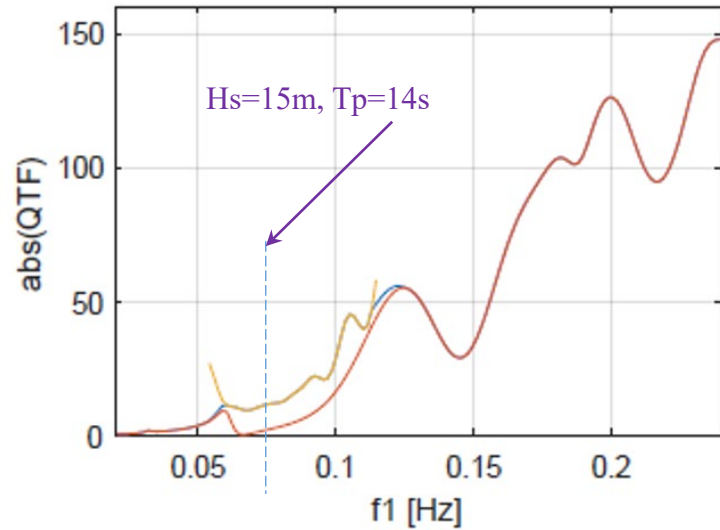
Large viscous drift
contribution at low
frequencies



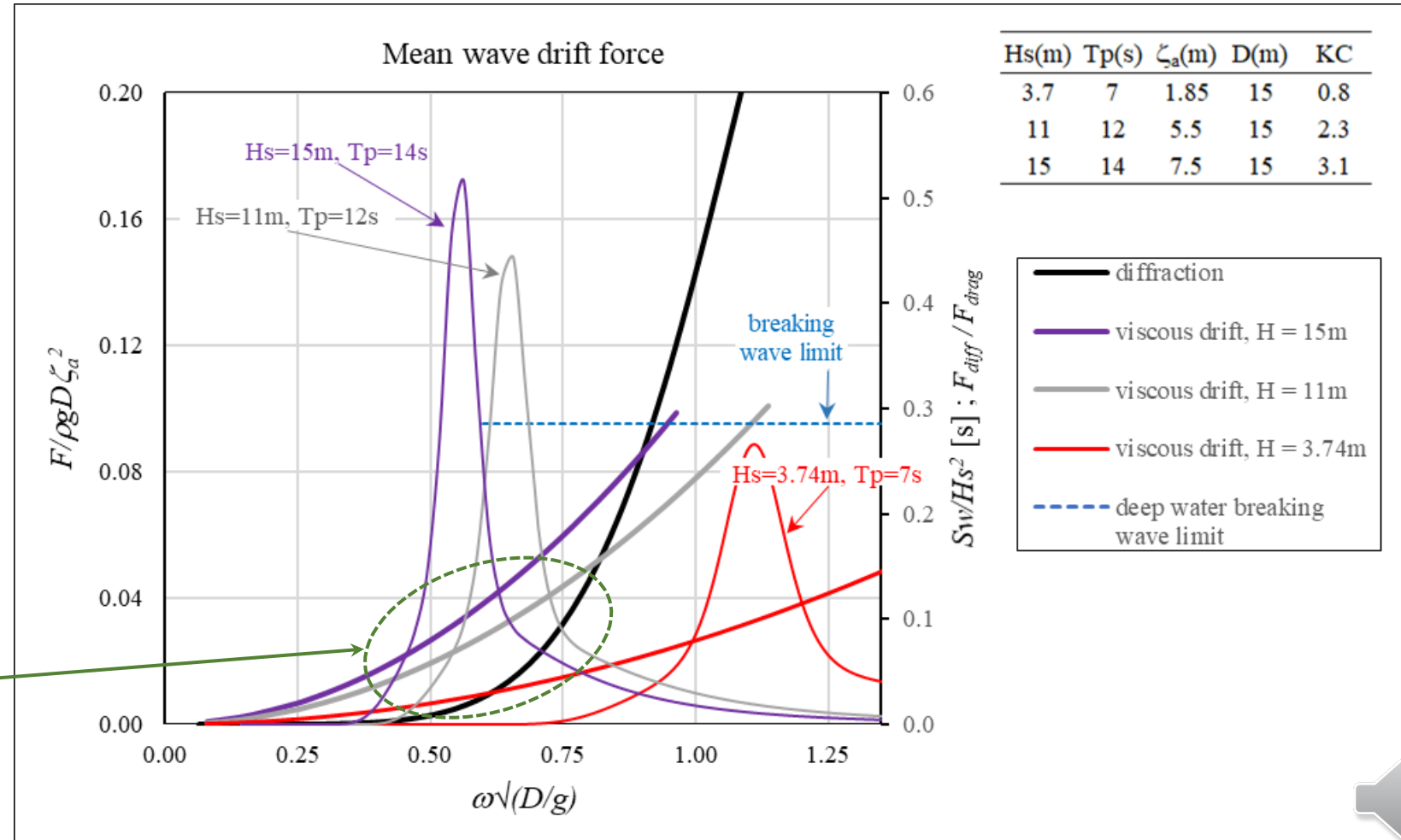
5. Results: discussion of empirical vs numerical QTFs

Mean drag force over one wave cycle
according to Morison's term with $C_d = 1.0$:

$$F_{drag} = (2/3\pi)\rho DC_D \zeta_a^3 \omega^2$$

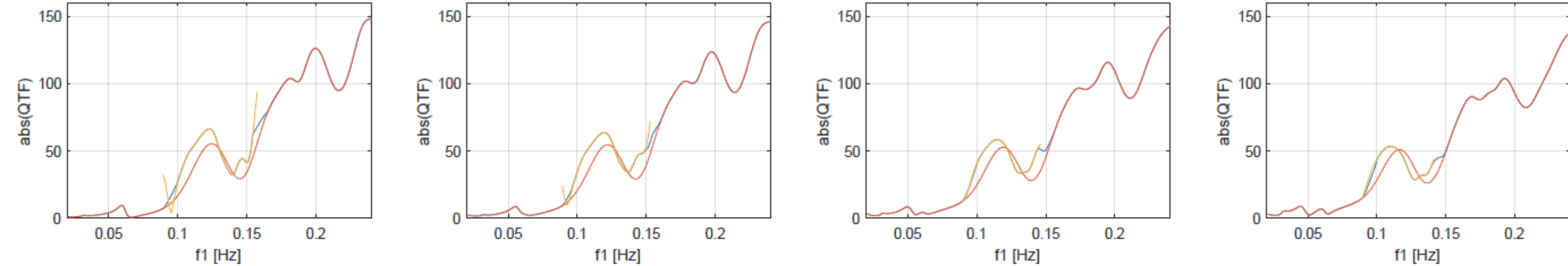


Large viscous drift
contribution at low
frequencies

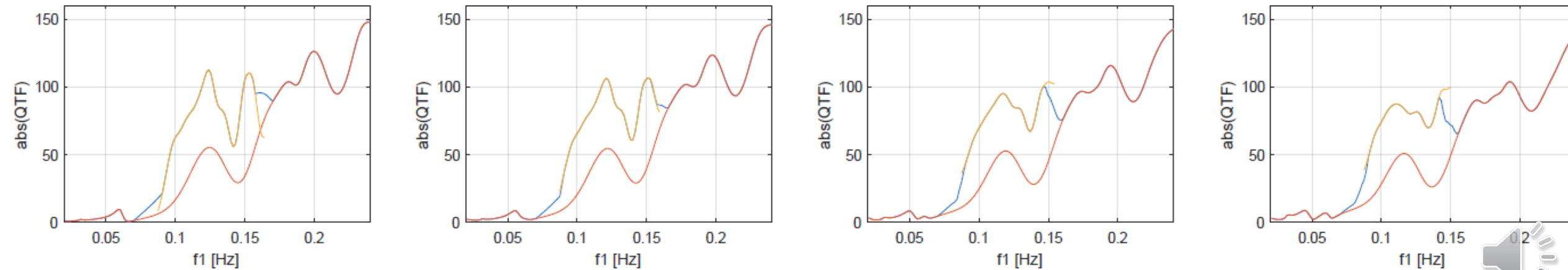


5. Results - effect of current ($H_s = 6.2$ m, $T_p = 9$ s, $U_c = 0$ and 1.2 m/s, Heading = 0 deg)

Force in X-dir, Direction = 0 deg., Test nr. = 4230 to 4244 $U_c = 0$

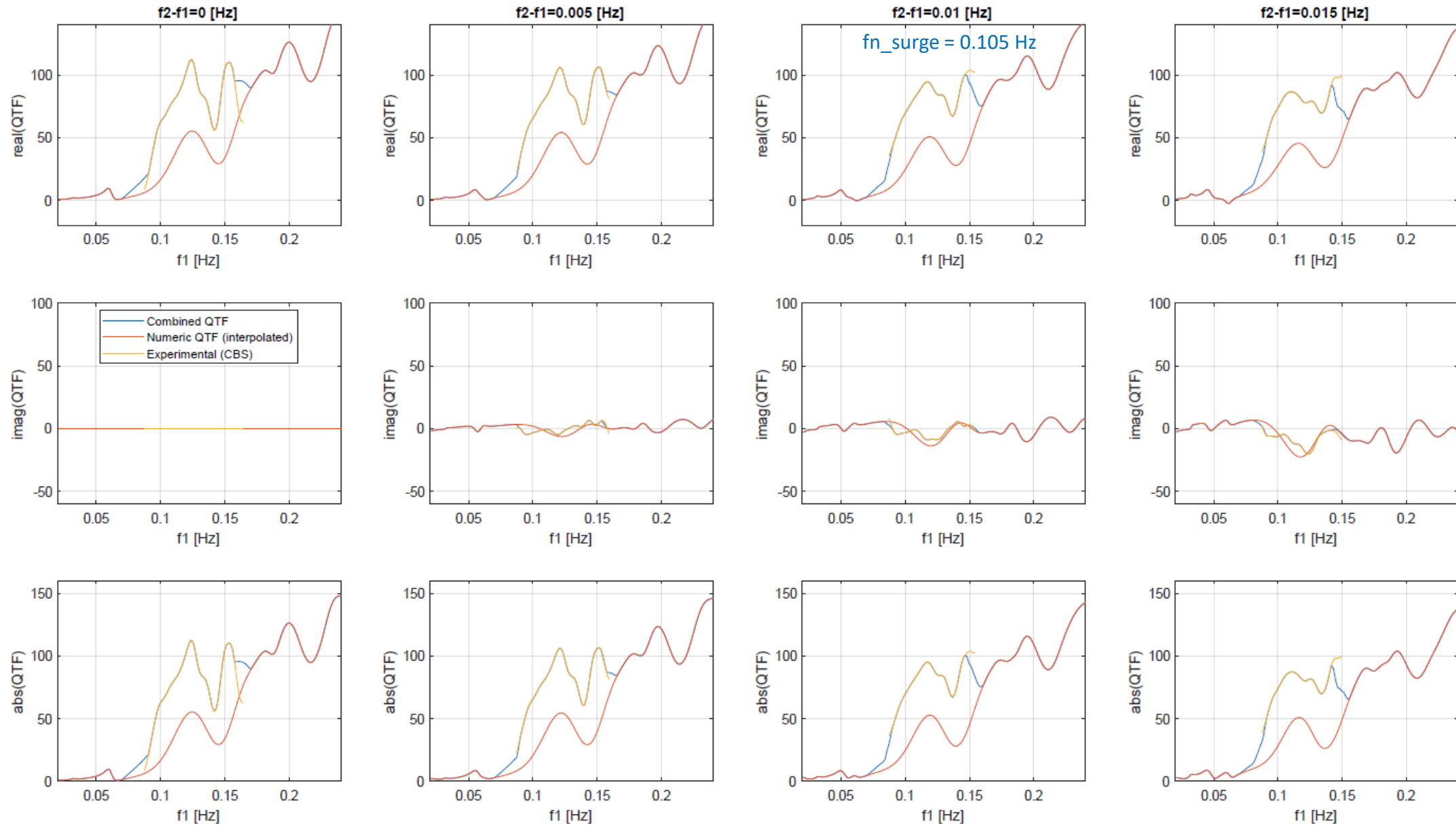


Force in X-dir, Direction = 0 deg., Test nr. = 4250-4263 $U_c = 1.2$ m/s



5. Results: effect of current ($H_s = 6.2$ m, $T_p = 9$ s, $U_c = 1.2$ m/s, Heading = 0 deg)

Force in X-dir, Direction = 0 deg., Test nr. = 4250-4263



6. Conclusions

Surge/Sway

- 2nd order potential flow calculations predict well the QTFs of low frequency wave loading in small seastates without current.
- 2nd order predictions underestimate the QTFs in moderate and high seastates, especially at the LF range (below around 0.1 Hz). Viscous drift is believed to be the root cause.
- Current effects result in a large increase of the QTF, which is observed for all diagonals.



Acknowledgement

The research leading to these results has received funding from the Research Council of Norway through the ENERGIX programme (grant 294573) and industry partners Equinor, MacGregor, Inocean, APL Norway and RWE Renewables.

The authors are grateful for the permission to use the INO WINDMOOR semisubmersible, which is jointly designed by Inocean and Equinor.